Homotopy Preserving Approximate Voronoi Diagram of 3D Polyhedron

Avneesh Sud [†]

Liangjun Zhang [‡]

Dinesh Manocha [§]

Department of Computer Science
University of North Carolina at Chapel Hill

Abstract

We present a novel algorithm to compute a homotopy preserving bounded-error approximate Voronoi diagram of a 3D polyhedron. Our approach uses spatial subdivision to generate an adaptive volumetric grid and computes an approximate Voronoi diagram within each grid cell. Moreover, we ensure each grid cell satisfies a homotopy preserving criterion by computing an arrangement of 2D conics within a plane. Homotopy equivalence implies a one-to-one correspondence between various topological components of the approximate Voronoi diagram and the exact Voronoi diagram. Our algorithm also satisfies Hausdorff distance bounds between the approximate and the exact Voronoi diagrams. We use distance based culling techniques to reduce number of non-linear arrangement computations and accelerate the computation. In practice, our algorithm can compute an approximate Voronoi diagram of complex models with thousands of primitives in tens of seconds.

1. Introduction

Given a set of geometric objects (called sites) and a distance function, the Voronoi diagram is a subdivision of the space into cells, such that all points in a cell have the same closest site according to the distance function. The Voronoi diagram is a fundamental geometric data structure and has been widely studied in computational geometry [Aur91, Sug92].

In this paper, we address the problem of computing the Voronoi diagram of a 3D polyhedron based on Euclidean distance function. Un4der the Euclidean distance metric, the Voronoi diagram of a polyhedral object is also closely related to its medial axis. The medial axis is a well defined skeletal representation that provides useful information about the shape and its topology. Voronoi diagrams and medial axes have been used for a number of applications, including computer vision and medical imaging [PSS*03], motion planning and navigation [FGLM01], mesh generation and finite element analysis [SERB98, Sur03], solid modeling [BBGS99], design and interrogation [PG90, Wol92], collision detection and proximity queries [LM03, SGG*06], and shape simplification [TH03].

The Voronoi diagram of a polyhedron can be represented using sheets, seams and junctions. Moreover, the sheets, seams and junctions of the Voronoi diagram of a polyhedral model have algebraic degree two, four and eight, respectively. Also the combinatorial complexity of the Voronoi diagram can be high - the upper bound is between $O(n^2)$ and $O(n^3 + \varepsilon)$ for any positive ε, where n is the number of faces, edges and vertices on the polyhedron [SA95]. As a result, the exact algorithms for computing the Voronoi diagrams can only handle polyhedron composed of a few hundred or thousand features [SPB96, CKM04]. Moreover, these algorithms cannot handle degenerate configurations and are susceptible to

---

[†] sud@cs.unc.edu

[‡] zlj@cs.unc.edu

[§] dm@cs.unc.edu

robustness problems. Many techniques have also been proposed to compute approximate Voronoi diagrams. At a broad level, these methods can be classified into point-sampling techniques [ABE04, ACK01, Boi86] and spatial subdivision algorithms [VO98, TT97, ER02, SOM04]. In practice, these algorithms are relatively simple to implement and can handle complex polyhedra. However, they may not provide topological guarantees on the computed approximation. Topological accuracy is desirable for certain applications of the Voronoi diagram. In particular, it has been shown that a bounded polyhedron is homotopy equivalent to its medial axis [Lie03]. Hence the topological properties of a polyhedron can be analysed by computing a homotopy-preserving medial axis.

Main Results: In this paper, we present an approach to compute an approximate Voronoi diagram that is homotopy equivalent to the exact Voronoi diagram. Homotopy equivalence enforces a one-to-one correspondence between the connected components, holes, tunnels or cavities and the way they are related in the exact Voronoi diagram and the computed approximation. Our approach is based on a spatial subdivision scheme and performs simple and efficient tests to compute a simplification of the exact Voronoi diagram. Moreover, we also describe algorithms to perform topological tests to guarantee homotopy equivalence of the approximate Voronoi diagram. Finally, we also provide Hausdorff distance bounds on the geometric structure of the approximate Voronoi diagram.

Thus, the homotopy-preserving approximate Voronoi diagram is useful for applications that exploit the topological structure of the Voronoi diagram. Such applications include homotopy-preserving medial axis computation [SFM05], motion planning [FGLM01], topology preserving simplification [SS06], shape analysis and feature identification [BPA01]. Along with hausdorff distance bounds, the approximate Voronoi diagram can be used for accelerating nearest neighbor and other proximity queries [SGG*06].Some of the main benefits of our approach include:

- **Topological properties**: We exploit topological properties of the Voronoi diagram of a polyhedral model, and use simple tests to guarantee homotopy equivalence between the computed approximate Voronoi diagram and the exact Voronoi diagram.

- **Computing arrangement of 2D conic sections:** Our topological tests reduce to computing an arrangement of 2D conic sections on a plane, instead of computing an arrangement of 3D quadric surfaces. The arrangement of 2D conics has been well studied and good implementations are available [KCMh99, Be05]. As a result, our algorithm is relatively simple to implement as compared to exact 3D Voronoi diagram computation algorithms and is less susceptible to robustness problems.

- **Handling near-degenerate configurations**: Our algorithm can provide topological guarantees even in presence of near-degenerate configurations of the the Voronoi diagram.

We have implemented our algorithm on a PC with 2.4Ghz AMD Opteron processor and applied it to complex CAD models consisting of thousands of primitives. Our algorithm is able to compute a homotopy preserving approximate Voronoi diagram of these models in tens of seconds. We also use the approximate Voronoi diagram to compute a simplified medial axis of the original model and give similar topological guarantees on the medial axis.

Organization: The rest of the paper is organized in the following manner. We give a brief overview of previous work in Section 2. We present the background material and an overview of our algorithm in Section 3. In Section 4, we present some topological properties of the Euclidean Voronoi diagram and our homotopy preserving criterion. Our subdivision algorithm is presented in Section 5. We describe its implementation and present results in Section 6. Finally, we analyze our algorithm and compare it with other approaches in Section 7.

2. Related Work

The problem of Voronoi diagram computation is well studied in computational geometry, solid modeling and their applications. In this section, we give a brief overview of previous algorithms. Previous work on computation of the Voronoi diagram and the medial axis of 3D shapes can be categorized based on the sampling of $\mathbb{R}^3$. The discretization based methods approximate either the boundary of a polyhedral model with finite point samples, or sample the domain inside the polyhedron using spatial subdivision. The analytic methods trace the components of the Voronoi diagram using algebraic techniques.

2.1. Discretization based methods

Voronoi Graph of finite point samples: These methods approximate the boundary of the 3D polyhedron by a finite set of points and compute the Voronoi graph. Robust and efficient methods for computing the Voronoi diagram of point samples are well known. We refer the reader to a survey by [AK00]. The Voronoi graph of a finite set of points provides an approximation to the exact Voronoi diagram of the polyhedron [ACK01]. The convergence to the exact Voronoi diagram has been shown for a sufficient dense sampling of smooth shapes. However, these methods algorithms may fail to provide a high quality approximation near sharp features of the original. Dey and Zhao [DZ02] present an algorithm to approximate Voronoi diagrams and also give a convergence guarantee.

Spatial Subdivision techniques: These methods subdivide the space into cells and compute an approximate Voronoi diagram of a polyhedral model. The key step common to these algorithms is to compute and label each cell with a set of Voronoi governors and compute an approximate arrangement of Voronoi elements inside each cell. Vleugels and Overmars [VO98] present a technique to compute an approximate Voronoi diagram by determining cells that lie near Voronoi region boundaries. Approaches to efficiently perform labeling of a cell using propagation techniques have been presented for tetrahedral [TT97] and octree grids [BCMS05]. Etzion and Rappoport [ER02] decouple the computation of the symbolic part (the topology) of the Voronoi diagram from the geometric part and trace Voronoi elements across cell boundaries. Stolpner and Siddiqui [SS06] identify cells containing points on the medial axis using the average flux of the distance field gradient through the boundary of the cell and use this property for guiding the subdivision. We provide more detailed comparison with these approaches in Section 7.

There is also work on computing a discrete approximation to the Voronoi diagram by sampling the domain on a uniform grid. In such methods, the Voronoi regions are approximated using a finite set of points along a uniform grid. These approaches are well suited for interactive computation using graphics hardware [HCK*99, Den03, SOM04].

However, previous spatial subdivision approaches cannot provide topological guarantees and may require extremely high level of subdivision to resolve near degenerate configurations in the Voronoi diagram.

2.2. Analytic methods

These methods detect topological events in the structure of the Voronoi diagram by tracing through a continuous domain. The correctness of continuous methods are not restricted by sampling parameters. Rather, these algorithms trace the 3D Voronoi edges (seams) [Mil93, SPB96, RT95]. The approaches are highly sensitive to numerical precision. While robust 2D implementations have been presented [Hel01], robust 3D implementations are difficult since it requires solving systems of tri-variate non-linear equations. In presence of degenerate configurations of the Voronoi diagram, such algorithms may fail to produce a valid output. A technique based on exact curve tracing is presented in [CKM04], however it does not scale well to large models. Furthermore, extremely high arithmetic precision is required to resolve near-degenerate configurations.

2.3. Topological Approximations

Under the Euclidean distance metric, the concept of Voronoi diagram is also closely related to the medial axis of a polyhedron. In particular, given a homotopy preserving approximation of a Voronoi diagram, Sud et al. [SFM05] present

an algorithm to compute a homotopy preserving simplified medial axis of a polyhedral model. Hence the homotopy preserving approximate Voronoi diagram can be used as an input for their work. Attali, Boissonat, and Edelsbrunner [ABE04] survey different techniques that generate a stable and homotopy preserving medial structure. The homotopy relationship between an object and its medial axis has been proven in a particularly general form by Lieutier [Lie03], who shows that homotopy preservation holds for any bounded open subset of $\mathbb{R}^n$. Chazal and Soufflet [CS04] present smoothness constraints on the boundary of a solid, which need not be polyhedral, under which the medial axis obeys certain stability and finiteness conditions. Chazal and Lieutier [CL04] have also proven results about stability, and present a homotopy preserving medial axis simplification.

3. Overview

In this section, we introduce some of the terminology used in the rest of the paper and provide an overview of our approach.

3.1. Terminology

The detailed notation used in the paper is summarized in Table 3.1. We explain some of those terms below.

Notation	Meaning
$\overline{\mathcal{X}}$	Closure of a set $\mathcal{X}$
$\mathcal{X}^c$	Complement of $\mathcal{X}$
$\text{Int}(\mathcal{X})$	Interior of $\mathcal{X}$
$\partial\mathcal{X}$	Boundary of $\mathcal{X}$
$|\mathcal{X}|$	Cardinality of $\mathcal{X}$
$\mathcal{O}$	A polyhedral solid in $\mathbb{R}^3$
p_i	A face, edge or vertex site in $\mathbb{R}^3$
$car(p_i)$	*Carrier* of a site p_i
$d(\mathbf{q},\mathbf{p})$	Distance between points $\mathbf{q}$ and $\mathbf{p}$
$d(\mathbf{q},p_i)$	Distance between a site p_i and point $\mathbf{q}$
	$d(\mathbf{q},p_i) = \min_{\mathbf{p}\in p_i}(d(\mathbf{q},\mathbf{p}))$
$\pi_{p_i}(\mathbf{q})$	*Projection* of a point $\mathbf{q}$ on a site p_i
$\mathcal{X} \sim \mathcal{Y}$	Sets $\mathcal{X}$, $\mathcal{Y}$ are homotopy equivalent
$\mathcal{X} \cong \mathcal{Y}$	Sets $\mathcal{X}$, $\mathcal{Y}$ are homeomorphic
B^d	A topological ball in d dimensions
S^d	A topological d-sphere in $d+1$ dimensions

Table 1: *This table highlights the notation used in the paper*

Given a closed polyhedral solid $\mathcal{O}$ in 3D, its boundary $\partial\mathcal{O}$ can be decomposed disjointly into vertices, open edges, and open faces, which we refer to collectively as *sites*. We shall denote the set of sites in $\partial\mathcal{O}$ as $\mathcal{A}$.

The *carrier* of an edge (face) site is the infinite line (plane) containing the site. The carrier of a vertex site is the vertex

itself. The *projection* of a point $\mathbf{q}$ on a site p_i, represented as $\pi_{p_i}(\mathbf{q})$, is the closest point on the the the site p_i to the point $\mathbf{q}$:

$$\pi_{p_i}(\mathbf{q}) = \{\mathbf{x} \in p_i \mid d(\mathbf{q},\mathbf{x}) \leq d(\mathbf{q},p_i)\},$$

where $d()$ is the distance function.

The closed Voronoi region of a site p_i is defined as:

$$\mathcal{V}(p_i) = \overline{\mathcal{X}}, \text{ where } \mathcal{X} = \{\mathbf{q} \mid d(\mathbf{q},p_i) < d(\mathbf{q},p_j) \forall p_j \in \mathcal{A}\}.$$

For each point $\mathbf{x}$, we define the set of *governors*, $\mathcal{G}(\mathbf{x})$, to be the set of sites for which $\mathbf{x}$ belongs to the closed Voronoi region.

$$\mathcal{G}(\mathbf{x}) = \{p_i \mid \mathbf{x} \in \mathcal{V}(p_i), p_i \in \mathcal{A}\}$$

The governor set of a set of points is the union of governors of each point. Let α denote a set of two or more sites. The boundary of the Voronoi region is composed of bisectors with other sites called Voronoi faces. A *Voronoi face or a sheet*, denoted f_α, is a maximally connected 2-manifold surface which has the same 2 governors, i.e. $|\alpha| = 2$. The 2-D Voronoi faces meet in maximally connected 1-manifold curves called *Voronoi edges or seams*, which have the same set of governors. Each Voronoi edge has 3 or more governors. A Voronoi edge is denoted $e_\alpha, |\alpha| \geq 3$. Finally, the Voronoi edges meet at points called *Voronoi vertices or junctions* which are equidistant from four or more sites. A Voronoi vertex is denoted $v_\alpha, |\alpha| \geq 4$. The set of all Voronoi faces, edges and vertices is the generalized Voronoi diagram of $\mathcal{A}$, represented as $\mathcal{VD}(\mathcal{A})$ [AK96]. Formally,

$$\mathcal{VD}(\mathcal{A}) = \bigcup_{p_i,p_j \in \mathcal{A}, i \neq j} \mathcal{V}(p_i) \cap \mathcal{V}(p_j).$$

The Voronoi diagram decomposes the space into Voronoi regions. For each point $\mathbf{x} \in \mathcal{V}(p_i)$, $|\mathcal{G}(\mathbf{x})| = 1$. The Voronoi faces, edges and vertices are collectively called the elements of the Voronoi diagram.

We use the formulation described in [ER02] and define the Voronoi graph $VG(\mathcal{A})$ as an undirected graph with the following properties:

1. Each node in $VG(\mathcal{A})$ corresponds to a Voronoi element (face, edge or vertex).

2. Two nodes in $VG(\mathcal{A})$ share an arc iff there is an incidence relationship between the two corresponding Voronoi elements.

3. Each node is labeled by the governor set of its corresponding elements.

The Voronoi graph encodes the symbolic part of the Voronoi diagram. Our algorithm computes an approximate Voronoi graph. The approximate Voronoi graph computed by our algorithm has the following additional property: a node in the approximate Voronoi graph replaces a sub-graph in the

exact Voronoi graph such that the corresponding approximate Voronoi diagram is homotopy equivalent to the exact Voronoi diagram.

A cell in the spatial subdivision of the space is denoted C, and is homeomorphic to a closed ball B^3. The elements of a cell are the cell faces, edges and vertices. For a cell C, $\mathcal{G}(C)$ is the set of sites whose Voronoi regions intersect C. A cell C is called a *boundary* cell if $C \cap \mathcal{A} \neq \emptyset$, i.e. the cell intersects one or more sites. A cell which is not a boundary cell is called an *interior* cell.

3.2. Homotopy Equivalence

The notion of homotopy equivalence between topological sets enforces a one-to-one correspondence between connected components, holes, tunnels or cavities. Formally, two maps $f: \mathcal{X} \to \mathcal{Y}$ and $g: \mathcal{X} \to \mathcal{Y}$ are *homotopic* if there exists a continuous family of maps $h_t: \mathcal{X} \to \mathcal{Y}$, for $t \in [0,1]$, such that $h_0 = f$ and $h_1 = g$. Thus, a homotopy is a deformation of one map to another. Two spaces $\mathcal{X}$ and $\mathcal{Y}$ are *homotopy equivalent* if there exist continuous maps $f: \mathcal{X} \to \mathcal{Y}$ and $g: \mathcal{Y} \to \mathcal{X}$ such that $g \circ f$ and $f \circ g$ are homotopic to the identity maps on their respective spaces. As an example, f could be the inclusion of a circle into an annulus, and g could be radial projection of the annulus onto the circle.

In situations such as this one, where f is an inclusion and $f \circ g$ is actually equal to the identity map, the homotopy equivalence is called a *deformation retraction*. See Spanier [Spa89] for details of these definitions. Our approximate Voronoi computation algorithm *implicitly* performs a sequence of deformation retractions on the exact Voronoi diagram to generate a simplified Voronoi diagram with the same homotopy type as the original.

3.3. Overview

We now provide an overview of our approach for computing the homotopy preserving approximate Voronoi diagram of a 3D polyhedron. We assume that the Voronoi diagram is defined with respect to the Euclidean metric. We construct the Voronoi diagram by separately computing the symbolic and geometric parts. We compute an approximate Voronoi graph, such that the corresponding approximate Voronoi diagram is homotopy equivalent to the exact Voronoi diagram.

The computation of the symbolic part of the Voronoi diagram is based on spatial subdivision that is used to compute the incidence relationships between Voronoi diagram elements. During spatial subdivision, each cell and the cell elements are labeled by their respective governors. The subdivision is terminated when the portion of the Voronoi diagram constrained to the interior of the cell is homotopy equivalent to a point. Under this condition, multiple vertex nodes in the Voronoi graph inside the cell can be replaced by a single vertex node. An example is shown in figure 1.
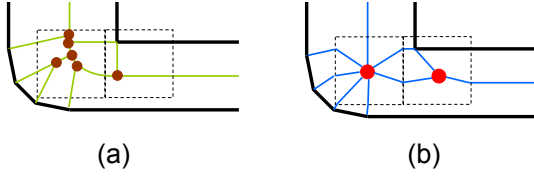
Figure 1: *Homotopy Preserving Approximate Voronoi Diagram: A subset of a 2D polygon is shown in bold. (a) The exact Voronoi diagram is shown in green. Two cells of a spatial subdivision are shown with dotted lines. Brown points represent Voronoi vertex nodes. (b) Each cell satisfies the homotopy preserving criterion. The corresponding homotopy preserving approximate Voronoi graph is shown in blue. The red points represent nodes approximating the Voronoi subgraph inside the cell.*

To guarantee homotopy equivalence, we first highlight some topological properties of Voronoi regions under the Euclidean distance metric. Moreover, we present a criterion to guarantee that the Voronoi diagram computed within a cell is homotopy equivalent to a point. The criterion is based on computing the arrangement of conics (i.e. degree two algebraic curves) on a plane and involves solving univariate quartic equations. The criterion is presented in Section 4. In order to accelerate the computation and reduce the number of non-linear tests, we perform spatial subdivision and update the governor set associated with each cell. The algorithms to evaluate the homotopy criteria and computing a homotopy preserving approximate Voronoi graph are presented in Section 5.

Given the graph of homotopy preserving approximate Voronoi diagram, we compute a geometric approximation to the Voronoi diagram using techniques presented in [ER02, BCMS05]. This involves computing an approximation of the seams and sheets. Furthermore, the diameter of the cell used for spatial subdivision algorithm provides bounds on the two sided Hausdorff distance between the geometric approximation and the exact Voronoi diagram. In other words, the cell size is chosen as a function of the Hausdorff bound.

In our approach, we ignore degenerate Voronoi regions. A Voronoi region $\mathcal{V}(p_i)$ is said to be degenerate if it has zero volume, i.e. there does not exist an open ball B^3 such that $B^3 \subset \mathcal{V}(p_i)$. Such Voronoi regions belong to an edge shared between two co-planar triangles, or a vertex for which all incident triangles are co-planar. Sites with degenerate Voronoi regions are removed from $\mathcal{A}$ as a preprocess. Note that removal of degenerate Voronoi regions does not change the homotopy type of the Voronoi diagram, since a degenerate Voronoi region is a subset of the closure of an adjacent Voronoi region. Furthermore, we constrain the domain of computation to be inside a bounding box of the polyhedron, so that each Voronoi region is closed and bounded (i.e. it is a compact set).

4. Homotopy Preserving Voronoi Diagram

In this section, we present our theoretical results and subdivision criteria to guarantee homotopy equivalence between the approximate Voronoi diagram and the exact Voronoi diagram in a cell. We use this criteria as part of the algorithm presented in Section 5.

We begin by enumerating a topological property of Euclidean Voronoi regions and then introduce the criteria used to guarantee homotopy equivalence. Finally, we show that our criteria are satisfied at some finite level of subdivision, and thereby proving completeness.

Property 1 (Voronoi regions are topological balls) If each site p_i is a convex set, then each bounded Voronoi region $\mathcal{V}(p_i)$, under the Euclidean distance metric, is homeomorphic to an open ball B^3.

Proof We show that $\mathcal{V}(p_i)$ is contractible, i.e. homotopy equivalent to a point in $\mathbb{R}^3$. and rely on the fact that a contractible compact subset of $\mathbb{R}^3$ is homeomorphic to a ball B^3 [CZ06]. We prove contractibility by constructing an explicit map. We define a continuous map $F : \mathcal{V}(p_i) \times I \rightarrow \mathcal{V}(p_i)$, such that $F(\mathbf{x}, 0) = \mathbf{x}$, for any $\mathbf{x} \in \mathcal{V}(p_i)$, and $F(\mathbf{x}, 1) = \mathbf{c}$ for some point $\mathbf{c}$. Here I is the unit interval $[0, 1]$. Let $I_1 = [0, 0.5], I_2 = [0.5, 1]$. We construct F in two stages,

$$F(\mathbf{x}, t) = G(\mathbf{x}, t) \forall t \in I_1$$
$$= H(G(\mathbf{x}, 0.5), t) \forall t \in I_2$$

where, $G : \mathcal{V}(p_i) \times I_1 \rightarrow \mathcal{V}(p_i)$ and $H : p_i \times I_2 \rightarrow p_i$, $G(\mathcal{V}(p_i), 0.5) \subseteq p_i$ and $H(p_i, 1) = \mathbf{c}$.

First we shall construct G. Consider the map $\pi_{p_i}(\mathbf{x}) : \mathcal{V}(p_i) \rightarrow p_i$. Let $G(\mathbf{x}, t) = (1 - 2t)\mathbf{x} + 2t\pi_{p_i}(\mathbf{x})$, where $t \in I_1, \mathbf{x} \in L$. To prove that G is continuous, we need to show that $\pi_{p_i}(\mathbf{x})$ is continuous. Assume that $\pi_{p_i}(\mathbf{x})$ is not continuous. Then some point $\mathbf{x} \in \mathcal{V}(p_i)$ has 2 unique closest points on p_i, let $\pi_{p_i}(\mathbf{x}) = \{\mathbf{p_1}, \mathbf{p_2}\}$. Consider the isosceles triangle $\Delta \mathbf{x} \mathbf{p_1} \mathbf{p_2}$ and the mid-point, $\mathbf{p} = \frac{\mathbf{p_1} + \mathbf{p_2}}{2}$. Then $\overline{\mathbf{xp}}$ is an altitude from $\mathbf{x}$ to $\overline{\mathbf{p_1 p_2}}$ and $d(\mathbf{x})\mathbf{p} < d(\mathbf{x})\mathbf{p_1} = d(\mathbf{x})\mathbf{p_2}$. Since p_i is convex, $\mathbf{p} \in p_i$ and leads to the contradiction $\pi_{p_i}(\mathbf{x}) = \mathbf{p}$. Thus the maps $\pi_{p_i}(\mathbf{x})$ and G are continuous. Further $G(\mathbf{x}, t)$ gives the shortest path from $\mathbf{x}$ to p_i. Sherbrooke et al. [She95] show that (a) the shortest path from a point on the Voronoi diagram (medial axis) to the closest site lies entirely inside the Voronoi region, and (b) the shortest paths from two points on the Voronoi diagram to the closest site can intersect only at the site. Thus $G(\mathbf{x}, t) \in \mathcal{V}(p_i)$ for all $\mathbf{x} \in \mathcal{V}(p_i), t \in I_1$, and $G(\mathbf{x_1}, t) \cap G(\mathbf{x_2}, t) = \emptyset$ for $\mathbf{x_1}, \mathbf{x_2} \in \mathcal{V}(p_i), \mathbf{x_1} \neq \mathbf{x_2}, t \in [0, 0.5)$.

Now we construct the map H. Let $\mathbf{c}$ be the centroid of p_i. Since p_i is convex, $\mathbf{c} \in p_i$. Let $H(\mathbf{x}, t) = 2(1 - t)\mathbf{x} + 2(t - 0.5)\mathbf{c}, t \in I_2, \mathbf{x} \in p_i$. $H(\mathbf{x}, t)$ is a continuous function, by definition. Since each site is simply connected, $H(\mathbf{x}, t) \in p_i$ for all $\mathbf{x} \in p_i, t \in I$. By definition, $F(\mathbf{x}, t)$ is continuous at $t = 0.5$. Thus $\mathcal{V}(p_i)$ is contractible. $\square$

4.1. Homotopy Criterion

We now present the 2D criteria to check if the Voronoi diagram inside a cell in the spatial subdivision is homotopy equivalent to a point.

Definition (Homotopy Criterion): An Axis Aligned Bounding Box (AABB) cell C, with governor set $\mathcal{G}(C)$, satisfies the *homotopy criterion* if $\mathcal{V}(p_i) \cap \partial C$ is homeomorphic to a topological disk B^2, for each $p_i \in \mathcal{G}(C)$.

We will show that the Voronoi diagram inside a cell satisfying the homotopy criterion is contractible (i.e. homotopy equivalent to a point). Following this result, all Voronoi vertices inside the cell can be replaced by a single vertex while preserving the homotopy type. We now present some results that follow from the homotopy criterion and prove that the Voronoi diagram in the cell is indeed contractible.

Lemma 1 Let C be a cell satisfying the homotopy criterion. For all $p_i \in \mathcal{G}(C)$, (a) $\mathcal{V}(p_i) \cap \partial C \neq \emptyset$, (b) $\partial \mathcal{V}(p_i) \cap C \cong B^2$ and (c) $\mathcal{V}(p_i) \cap C \cong B^3$.
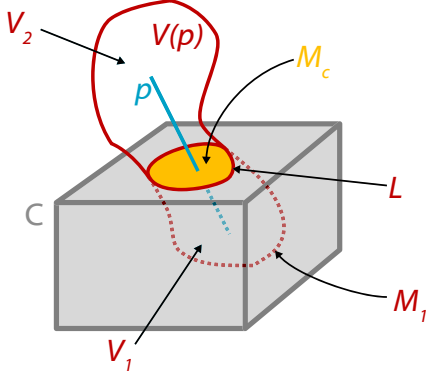
Figure 2: *Proof of Lemma 1: The Voronoi region $\mathcal{V}(p)$, of a line site p, intersecting a 3D cell C. The boundary of the cell partitions $\mathcal{V}(p)$ into 2 regions: V_1 in the interior of C and V_2 in the exterior. $\partial V_1 = M_1$. Intersection of $\mathcal{V}(site)$ with ∂C is a topological disk, denoted M_c*

Proof The result (a) follows from the definition of $\mathcal{G}(C)$. ∂C partitions $\mathcal{V}(p_i)$ into 2 spaces, $V_1 = \mathcal{V}(p_i) \cap C, V_2 = \mathcal{V}(p_i) \cap C^c$ (i.e. V_2 is outside the cell C). Let $M_1 = \partial \mathcal{V}(p_i) \cap \partial C, M_c = \mathcal{V}(p_i) \cap \partial C, L = \partial M_c = \partial \mathcal{V}(p_i) \cap \partial C$. We need to show that $M_1 \cong B^2, V_1 \cong B^3$. From the homotopy criterion, $M_c \cong B^2$, and the boundary L is a simple closed curve, $L \cong S^1$. This boils down to proving that $V_1 \cong B^3$. From property 1, it follows that $\partial \mathcal{V}(p_i) \cong S^2$. Furthermore, $L \subset \partial \mathcal{V}(p_i)$, and using the Jordan curve theorem on the 2-sphere, it partitions $\partial \mathcal{V}(p_i)$ into 2 topological disks. Thus, $M_1 \cong B^2$. We now define a homeomorphism $f : \partial M_1 \to \partial M_c$ which glues M_1 to M_c. We also have $M_1 \cap M_c = L \cong S^1$. Thus f is the identity map on L, which maps each point on ∂M_1 to the iden-

tical point on ∂M_c. Thus the connected sum of M_1 and M_c is homeomorphic to a 2-sphere. Then $M_1 \cup M_c \cong S^2$, thus $\partial V_1 \cong S^2, V_1 \cong B^3$. $\square$

Using the above results, we provide an explicit construction to prove that the homotopy criterion is sufficient for the Voronoi diagram constrained to the cell is contractible. To prove this, we perform a series of retractions on the Voronoi regions contained inside a cell.

We define a retraction $g_i : C \to C$ to be the exclusion of the interior of Voronoi region from the cell C (see figure 3). Given a cell C satisfying the homotopy criterion, let V_k be the subset of C left after k retractions, where $k = 0, 1, \ldots, |\mathcal{G}(C)|$. We now prove a result on the retractions.
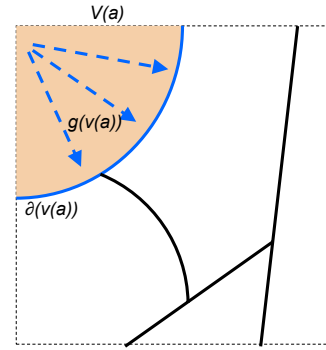
Figure 3: *Deformation retract of a Voronoi region: A 2D cell is shown with dotted boundary. The solid curves represent a Voronoi diagram. Each Voronoi region satisfies the homotopy criterion (in 2D). The retraction g takes all points in the Voronoi region $\mathcal{V}(a)$ to its boundary $\partial \mathcal{V}(a)$.*

Lemma 2 V_{k+1} is homotopy equivalent to V_k.

Proof $V_{k+1} = V_k \setminus \text{Int}(\mathcal{V}(p_i))$. Since C satisfies homotopy criterion, $\mathcal{V}(p_i) \cap C \cong B^3$ and $\partial \mathcal{V}(p_i) \cap C \cong B^2$. Also, $(\mathcal{V}(p_i) \cap C) \setminus \text{Int}(\mathcal{V}(p_i)) = \partial \mathcal{V}(p_i) \cap C$. There exists a deformation retract from a ball B^3 to a disc B^2. This implies existence of a map $G : \mathcal{V}(p_i) \cap C \to \partial \mathcal{V}(p_i) \cap C$ such that: (a) the restriction of H to $\partial \mathcal{V}(p_i) \cap C$ is equal to the identity on $\partial \mathcal{V}(p_i) \cap C$, and (b) $H \circ G$ is homotopic to the identity on $\partial \mathcal{V}(p_i) \cap C$, where H is the inclusion $\partial \mathcal{V}(p_i) \to \mathcal{V}(p_i)$.

We then define $\hat{G} : V_k \to V_{k+1}$ to be the identity on $V_{k+1} \subset V_k$ and equal to G on $\text{Int}(\mathcal{V}(p_i))$. Then if $\hat{H}$ is the inclusion $V_{k+1} \to V_k$, it is clear that $\hat{G} \circ \hat{H}$ is homotopic to the identity on V_k and $\hat{H} \circ \hat{G}$ is homotopic to the identity on V_{k+1}. Thus $V_k \sim V_{k+1}$. $\square$

Theorem 1 If a cell satisfies the homotopy criterion, then the Voronoi diagram constrained to the cell is contractible.

Proof Initially $V_0 = C$ and finally $V_f = \mathcal{VD}(\mathcal{A}) \cap C$ where

$f = |\mathcal{G}(C)|$. From lemma 2, V_0 and V_f are homotopy equivalent. We know that the cell C is contractible. Thus V_f is contractible. $\quad\square$

4.2. Completeness

In this section, we prove the completeness. To do this we use the following theorem:

Theorem 2 For any point on the boundary of a Voronoi region $\mathcal{V}(p_i)$, there exists an open ball B_r of strictly positive radius r such that $\partial\mathcal{V}(p_i) \cap B_r \cong B^2$.

Proof We perform case analysis on the location of the point.

(a) The point lies in the interior of a Voronoi face. Each face is a 2-manifold embedded in $\mathbb{R}^3$. Then at each point on the face, there exists an open ball of finite radius such that intersection of the ball with the face is 2-manifold - i.e. homeomorphic to a disk.

(b) The point lies in the interior of a Voronoi edge. At a Voronoi edge, the Voronoi region is bounded by 2 Voronoi faces. Each bisector surface (i.e. a quadric surface) is diffeomorphic to a disk. In a small neighborhood of the point, the arrangement of the Voronoi faces incident at the Voronoi edge is homeomorphic to the arrangement of a set of half-planes incident at an edge. The intersection of a half-plane with a sphere centered on the edge is a single curve segment. Then the 2 curve segments, arising from the intersection of the sphere and the two bounding Voronoi faces meet at exactly 2 points - the end points of the 2 curves. Thus the boundary of the intersection of Voronoi region boundary at a Voronoi edge and the boundary of ball (centered on edge) is a circle. Therefore, the intersection with the ball is a disk.

(c) The point lies on a Voronoi vertex. The proof for case (b) extends to this case. The boundary of a Voronoi region in the neighborhood of a vertex consists of a finite number of Voronoi faces meeting at Voronoi edges. $\quad\square$

Theorem 2 implies that for any point on the Voronoi diagram $\mathcal{VD}(\mathcal{A})$, we can find a ball of a finite radius such that the intersection of the Voronoi regions with the ball satisfy the homotopy criterion. Thus the subdivision will terminate once the current cell is contained inside such a ball.

5. Approximate Voronoi Diagram Computation

In this section, we present details of our algorithm. First we describe how we evaluate the homotopy criterion for each Voronoi region in a given cell. Then we present our algorithm to compute the graph of the approximate Voronoi region.

5.1. Homotopy Criterion Computation

Theorem 1 in Section 4 implies that this test reduces to checking whether the intersection of the Voronoi diagram with the boundary of a cell is homeomorphic to a disk. This is equivalent to determining if the intersection of the boundary of a Voronoi region with a cell is homeomorphic to a circle. We compute the boundary of the Voronoi region along each face of the cell and compute the union over all faces.

The boundary of a Voronoi region consists of sheets, seams and junctions. Each sheet is a subset of the bisector between the carriers of two sites. Given a sheet f_α and a cell face F, a *Voronoi face event* is the intersection of f_α and F and corresponds to a conic curve on F in the general case. We compute an arrangement of the conics on the face [KCMh99]. The intersection of the conic sections gives *Voronoi edge events* [ER02], representing intersection of seams with a cell face. Along with each edge event, we store the set of governors of the Voronoi edge. If the sheet is a plane tangential to cell face, we compute the intersection with the face vertices. In case the Voronoi edge event consists of infinite number of points, we compute its intersection with the boundary of a face.
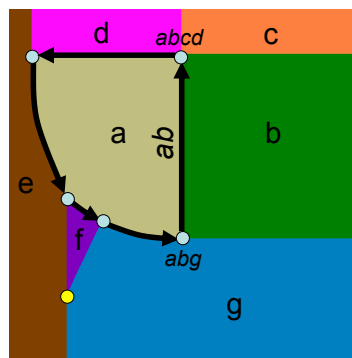
Figure 4: *Homotopy criterion computation: We show a face of a cell in the computation of approximate Voronoi diagram of the L-shape. Each colored region represents the intersection of a Voronoi region with the face, and is labeled by its governor. Each region is homeomorphic to a disc, hence satisfies the homotopy criterion. The circles represent Voronoi edge events: e.g. the point $(abcd)$ represents intersection of a degenerate Voronoi edge and the face. The bold conic segments represent the face events, representing boundary of the Voronoi region of site a, computed by our tracing algorithm.*

All intersections of conics do not provide the valid edge events. We compute the valid edge events based on the algorithm `CellFaceVoronoiEdgeIntersection` presented in [ER02]. Given the set of edge events, we trace the conic segments between edge events sharing a common governor to obtain the Voronoi face events. A closed sequence of face events sharing a common governor provides the boundary of the Voronoi region of the site on the cell face. Two edge events are connected by a face event if they share at least two common governors (corresponding to the bisector between the governors). In case there are multiple points
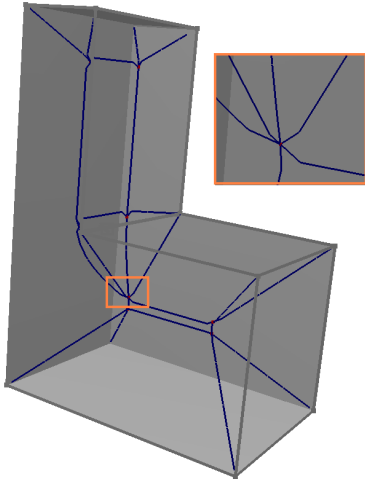
Figure 5: *L-shape Model: The homotopy preserving approximate Voronoi diagram is computed for this model. The edges of the approximate Voronoi diagram are shown in blue. The vertices are highlighted with red. The orange region shows a zoomed in view of a degenerate vertex with 6 seams incident on it.*

sharing same 2 governor labels, we sort them according to their parametric coordinates on the conic and connect the 2 closest points. In the presence of degenerate seams, each conic segment between two edge events may not represent a valid face event. Checking if a segment is a valid face event is equivalent to determining if it lies on the boundary of the Voronoi region of a site p_i. In order to perform this test, we enumerate all conic segments incident on an edge event and trace along the conic segment which is closer to the p_i than to all other governors of the edge event. Finally, we join the face events at boundaries of adjacent faces to compute the intersection of the Voronoi region with the boundary of the cell. A cell satisfies the homotopy criterion if all the Voronoi region boundaries on the cell boundary form one simple closed loop.

5.2. Computing cell governors

The homotopy criterion needs to be satisfied for all sites that belong to the governor set of a cell. Here we present our scheme to compute a set of governors of the cell. We use a sequence of culling tests to prune the set of governors of a cell. A site p_i can be removed from the governor set of a cell C of diameter δ if:

1. **Distance exclusion**: There exists another governor $p_j \in \mathcal{G}(C)$ such that centroid of C is closer to p_j and difference in distance is greater than δ.

2. **Polytope exclusion**: The domain polytope (a polytope bounding the Voronoi region of site p_i) does not intersect C.
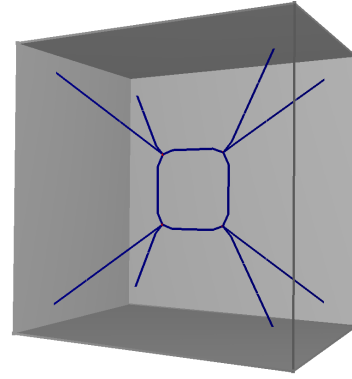
Figure 6: *Cuboid Model with 2 equal dimensions: The edges of the approximate Voronoi diagram are shown in blue. The vertices are highlighted with red.*

3. **Bisector exclusion**: There exists another governor $p_j \in \mathcal{G}(C)$ such the cell C is closer to p_j and lies inside the domain polytope of p_j.

Each of these tests involves solving inequalities or a system of linear equations [Cul00]. These tests provide a conservative estimate of the governors of a cell. The exact set of governors of the faces of a cell is computed from the arrangement of Voronoi regions on the faces, as described in section 5.1. We now present a result that ensures computing the arrangement on the boundary of a cell is sufficient for computing the cell governors.

Lemma 3 For an interior cell C, if $\mathcal{V}(p_j) \cap \mathrm{Int}(C) \neq \emptyset$ then $\mathcal{V}(p_j) \cap \partial C \neq \emptyset$.

The proof follows trivially from the facts that the Voronoi regions are connected (topological balls) and contain the site. A consequence of Lemma 3 is that it suffices to check the boundary of a cell to compute governors of an interior cell. For boundary cells, we impose further restrictions on the governor set of the cell to check if each Voronoi region intersects the cell boundary.

Boundary cell criterion: Given a boundary cell C, with a set of sites $\mathcal{X}$ intersecting C, C satisfies the boundary cell criterion if:

1. $\mathcal{X}$ contains at most one point site p_p, and $\mathcal{X} \setminus \{p_i\}$ contains sites incident on the point p_i.

2. The governor set $\mathcal{G}(C)$ is a subset of $\mathcal{X}$.

These two conditions ensure that each non point site in the governor set $\mathcal{G}(C)$ intersects the boundary of the cell - thus their Voronoi regions must intersect the boundary of the cell. For each point site, its Voronoi region constrained to the cell is given by intersection of its domain polytope and the cell, thus its Voronoi region must intersect the cell boundary if its domain polytope is non-empty. Condition (1) can be trivially tested. We conservatively test for condition (2) by checking

if the conservative governor set does not include any sites from $\mathcal{A} \setminus \mathcal{X}$.

5.3. Approximate Voronoi Diagram Computation

In this section we provide our algorithm for computing a homotopy preserving approximate Voronoi diagram. We first compute a homotopy preserving approximate Voronoi graph using spatial subdivision. The steps are given as follows:

1. Compute a discrete distance field on uniform grid at some fixed resolution.

2. Compute the governor set of each cell using exclusion tests presented in Section 5.2.

3. Check if a cell satisfies the homotopy criterion. In addition, check if each boundary cell satisfies the boundary criterion. If either of the criteria are not met, subdivide and update the governor sets of the children cells.

4. If a cell satisfies the homotopy and boundary criteria, insert a subgraph node inside the cell. Connect the node to the edge events on the boundary of the cell.

This algorithm provides us with a homotopy preserving approximate Voronoi graph. To extract the homotopy preserving approximate Voronoi diagram, we further refine it to detect unique vertex nodes and edge nodes. We use a result from [ER02] to detect Voronoi vertices: If the number of intersection points of a Voronoi edge e_α and ∂C is odd, then there exists a Voronoi vertex in C. We subdivide a leaf cell if it contains more than two edge events with same governor set. If a cell has exactly two edge events with same governor set, we remove the subgraph node and directly connect the two edge events with a subset of the Voronoi edge. The refined approximate Voronoi graph consists of nodes of type Voronoi vertex and subgraph and edge nodes connecting the vertex and subgraph nodes. We follow a loop of Voronoi edge events joined by the same face event on the boundary of a cell to extract the Voronoi faces.

6. Implementation and Results

In this section, we briefly describe our implementation and highlight its performance on different benchmarks. We have implemented the system in C++, and use OpenGL to display the results. The timings reported in this paper were taken on a 2.4Ghz Opteron PC with 1GB of memory. The discrete distance field and spatial grid is computed efficiently using graphics hardware [SGGM06]. The resolution of the uniform grid was chosen to be half of the length of the smallest edge of the polyhedron to ensure satisfiability of Condition (1) of the boundary criterion.

We have tested our algorithm on a set of examples from simple geometry with known degenerate configurations to more complex models consisting of thousands of sites. Figure 5 shows an L-bracket with symmetric cubical sections. The

bottom half contains degenerate seams and junctions. Figure 7) shows a spoon model with 254 sites. Figure 8) shows a flattened chisel model with a radial axis of symmetry and random perturbations added to the handle. This benchmark is particularly difficult to handle with many several degenerate configurations near the axis of the handle. As a result, there is a large governor set for many cells.
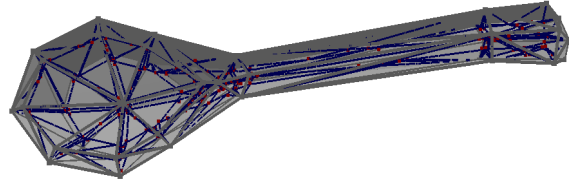
Figure 7: *Spoon Model: The model has 254 sites, including 84 triangle sites, 126 edge sites, and 44 vertex sites. The computation for homotopy preserving approximate Voronoi diagram took 1.7s for this model. The edges and vertices of the approximate Voronoi graph are highlighted in blue and red respectively.*
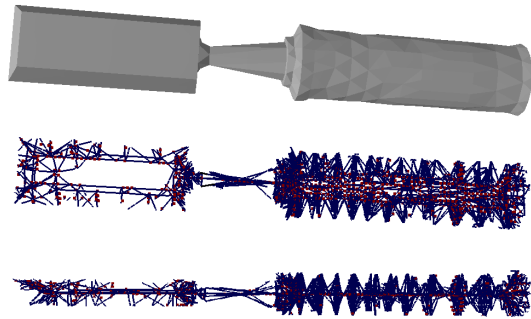
Figure 8: *Chisel Model: The model has $1,797$ sites, including 632 triangle sites, 847 edge sites, and 318 vertex sites. It has many degenerate configurations near the axis of the handle. Two views of the approximate Voronoi graph are shown in the bottom. The computation for homotopy preserving approximate Voronoi diagram took $130.3s$ for this model. The edges and vertices of the approximate Voronoi graph are highlighted in blue and red, respectively.*

6.1. Homotopy Preserving MAT Approximation

We have applied our homotopy preserving Voronoi diagram computation algorithm to compute a homotopy preserving medial axis approximation of 3D polyhedrons [SFM05]. In practice, this simplification tends to remove unstable features of Blum's medial axis, while preserving the topological structure. In particular, we can guarantee that the approximate medial axis is homotopy equivalent to the original shape. The approximate medial axis is extracted from

approximate Voronoi diagram by removing Voronoi faces with a governor set such that one governor is a subset of the closure of the other. The elements of the medial axis are removed using a stability measure based on the separation angle formed by connecting a point on the medial axis to its governors. Some examples of the computed homotopy preserving approximate medial axis are shown in figures 9- 10.

(a) Model   (b) Approximate MAT
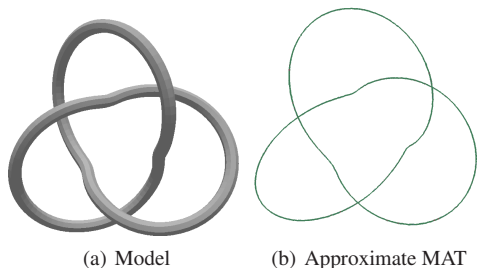
Figure 9: *Knot Model (2.5k polygons). The homotopy preserving Voronoi diagram is used to compute a homotopy preserving approximate medial axis (shown in green). The sheets consist of thin and long faces. The Voronoi diagram computation took* 5.2s.

7. Discussion

In this section we perform an analysis of the individual stages of our algorithm and compare it with prior techniques.

7.1. Analysis and Comparisons

The total running time of the subdivision algorithm is dependent on the depth of the subdivision performed and the relative configuration of the Voronoi faces. In this section, we provide time bounds on the computation cost per cell, specifically the cost of computing the homotopy criterion. Let the size of governor set of a cell be k. Then the number of intersection points is bounded by $O(k^2)$. Each intersection

(a) Model
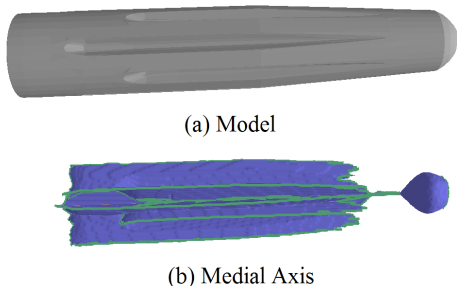
(b) Medial Axis

Figure 10: *Ridged Rod (5k polygons), The model has ridges near the surface, which leads to many unstable features in the medial axis. The sheets of the approximate medial axis are shown in (b). The Voronoi diagram computation took* 211s.

point is checked against remaining $O(k)$ governors to determine if it is a valid edge event. Given the set of edge events, they are sorted by their governor labels in $O(k^2 \log k^2)$ time. Next the algorithm used to trace the Voronoi edges in a single region boundary performs $O(1)$ computations at each edge event. Thus the total cost of computing the edge events and tracing the all Voronoi region boundaries on a cell is at most $O(k^3)$. Typically, the number of governors per cell is small, but in the worst case it can be $k = O(N)$, N = number of entities on the boundary) for degeneration configurations. The boundary criterion can be computed in $O(k)$ time.

Comparison: We compare our algorithm to prior approaches for computing the Voronoi diagram of polyhedral models.

The seam curve tracing methods [CKM04, SPB96, RT95] compute the exact Voronoi diagram. In practice, they can compute a topologically correct Voronoi diagram, but they require use of exact arithmetic to solve a system of tri-variate non linear equations. Furthermore, they are prone to degenerate configurations. As a result, these approaches may not scale well to large models.

Our work is most similar to work on computing an approximate Voronoi diagram using spatial subdivisionr. The work of [VO98, BCMS05, SS06] does not provide any topological guarantees on the computed approximate Voronoi diagram - instead the subdivision is carried out to a predefined level. The work of Etzion and Rappoport [ER02] provides a topologically valid Voronoi graph for cells of size greater than some predefined constant ε. In general, it is not easy to select a good value of ε for large models. For degenerate and near-degenerate configurations, they compute an approximate Voronoi graph, with no topological guarantees. In case of large cells, their approach computes an approximation that is homeomorphic to the exact Voronoi diagram only for non-degenerate configurations. Moreover, they require that the cells are subdivided till the number of governors of a cell is small (typically $4 - 6$, except for special cases). As a result, their approach can be rather conservative.

In comparison, our algorithm provides a less strict topological guarantee on the output. We ensure homotopy equivalence between the exact Voronoi diagram and our approximation, even in the presence of degenerate and near degenerate configurations. We exploit the fact that in the neighborhood of a near-degenerate configuration, the Voronoi diagram is homotopy equivalent to a point and this property simplifies the overall computation. The homotopy criterion, introduced in Section 4.1, also checks for this condition in a cell containing a degenerate configuration. Furthermore, the homotopy criterion allows for early termination during subdivision, even if a call has a large number of governors. This results in fewer levels of subdivision. In practice, the size of leaf nodes in the subdivision is of similar scale as the input geometry.

7.2. Limitations

Our algorithm has a few limitations. The approximate Voronoi diagram computed by our algorithm is not homeomorphic to the exact Voronoi diagram. Since it is based on spatial subdivision, the cost of computation and the complexity of the approximate Voronoi diagram varies based on the configuration the subdivision grid. In particular, one may encounter degenerate configurations in which the intersection of the Voronoi regions with the boundary of the cell may be a single point (i.e. a tangential intersection), and such cases cannot be easily resolved with only subdivisions. We believe a subdivision scheme which allows for perturbation of the cell faces may be able to alleviate this problem.

8. Conclusions and Future Work

We have presented an approach to compute a homotopy preserving approximate Voronoi diagram of a 3D polyhedron. Homotopy equivalence is a weaker topological guarantee compared to homeomorphism, however it captures all the topological features of the shape. Our algorithm is based on an adaptive spatial subdivision, and guarantees that the Voronoi diagram in each cell is homotopy equivalent to a point. The topological tests are performed by computing the arrangement of 2D conic sections.

Hence our algorithm is simpler than exact 3D Voronoi diagram computation and can handle near-degenerate configurations of the Voronoi diagram. We have highlighted its performance on many benchmarks and also used it to compute a homotopy preserving medial axis approximation.

There are many avenues for future work. The approximate homotopy preserving Voronoi diagram can have a complicated structure for large models. We would like to study various methods for simplifying this structure and apply it to different applications like motion planning, feature identification and shape analysis. Furthermore, we would like to evaluate the accuracy of those simplification schemes. We would also like to combine our algorithm to other subdivision schemes such as kd-trees, which offer a better choice of partitioning planes.

References

[ABE04] ATTALI D., BOISSONAT J.-D., EDELSBRUNNER H.: Stability and computation of the medial axis. In *Mathematical Foundations of Scientific Visualization, Computer Graphics, and Massive Data Exploration*. Springer-Verlag, 2004.

[ACK01] AMENTA N., CHOI S., KOLLURI R. K.: The power crust. In *Proc. ACM Symposium on Solid Modeling and Applications* (2001), pp. 249–260.

[AK96] AURENHAMMER F., KLEIN R.: *Voronoi Diagrams*. Tech. Rep. 198, Department of Computer Science, FernUniversität Hagen, Germany, 1996.

[AK00] AURENHAMMER F., KLEIN R.: Voronoi diagrams. In *Handbook of Computational Geometry*, Sack J.-R., Urrutia J., (Eds.). Elsevier Science Publishers B.V. North-Holland, Amsterdam, 2000, pp. 201–290.

[Aur91] AURENHAMMER F.: Voronoi diagrams: A survey of a fundamental geometric data structure. *ACM Comput. Surv. 23*, 3 (Sept. 1991), 345–405.

[BBGS99] BLANDING R., BROOKING C., GANTER M., STORTI D.: A skeletal-based solid editor. In *Proc. ACM Symposium on Solid Modeling and Applications* (1999), pp. 141–150.

[BCMS05] BOADA I., COLL N., MADERN N., SELLARES J. A.: Approximations of 3D generalized voronoi diagrams. In *Proc. 21st European Workshop on Computational Geometry* (2005), pp. 163–166.

[Be05] BERBERICH E., ET AL.: Exacus: Efficient and exact algorithms for curves and surfaces. *Proc. of the 13th European Symposium on Algorithms* (2005).

[Boi86] BOISSONNAT J.-D.: Automatic solid modeler for robotics applications. In *Robotics Research: Third International Symposium. MIT Press Series in Artificial Intelligence.* (Cambridge, MA, 1986), MIT Press, pp. 65–72.

[BPA01] BONNASSIE A., PEYRIN F., ATTALI D.: Shape description of three-dimensional images based on medial axis. In *10th International Conference on Image Processing (ICIP)* (2001), pp. 931–934.

[CKM04] CULVER T., KEYSER J., MANOCHA D.: Exact computation of a medial axis of a polyhedron. *Computer Aided Geometric Design 21*, 1 (2004), 65–98.

[CL04] CHAZAL F., LIEUTIER A.: Stability and homotopy of a subset of the medial axis. In *Proc. ACM Symposium on Solid Modeling and Applications* (2004).

[CS04] CHAZAL F., SOUFFLET R.: Stability and finiteness properties of medial axis and skeleton. *Journal of Control and Dynamical Systems 10*, 2 (2004), 149–170.

[Cul00] CULVER T.: *Accurate Computation of the Medial Axis of a Polyhedron*. PhD thesis, Department of Computer Science, University of North Carolina at Chapel Hill, 2000.

[CZ06] CAO H.-D., ZHU X.-P.: A complete proof of the poincaré and geometrization conjectures of the Hamilton-Perelman theory of the Ricci flow. *Asian Journal of Mathematics 10*, 2 (06 2006), 165 – 498.

[Den03] DENNY M.: Solving geometric optimization problems using graphics hardware. In *Proc. of Eurographics* (2003).

[DZ02] DEY T. K., ZHAO W.: Approximating the medial axis from the Voronoi diagram with a convergence guarantee. In *European Symposium on Algorithms* (2002), pp. 387–398.

[ER02] ETZION M., RAPPOPORT A.: Computing

Voronoi skeletons of a 3-d polyhedron by space subdivision. *Computational Geometry: Theory and Applications 21*, 3 (March 2002), 87–120.

[FGLM01] FOSKEY M., GARBER M., LIN M., MANOCHA D.: A voronoi-based hybrid planner. *Proc. of IEEE/RSJ Int. Conf. on Intelligent Robots and Systems* (2001).

[HCK*99] HOFF K., CULVER T., KEYSER J., LIN M., MANOCHA D.: Fast computation of generalized voronoi diagrams using graphics hardware. *Proceedings of ACM SIGGRAPH 1999* (1999), 277–286.

[Hel01] HELD M.: Vroni: An engineering approach to the reliable and efficient computation of Voronoi diagrams of points and line segments. *Computational Geometry: Theory and Applications 18* (2001), 95–123.

[KCMh99] KEYSER J., CULVER T., MANOCHA D., HNAN S. K.: MAPC: A library for efficient and exact manipulation of alge braic points and curves. In *Proc. 15th Annual ACM Symposium on Computational Geometry* (1999), pp. 360–369.

[Lie03] LIEUTIER A.: Any open bounded subset of R^n has the same homotopy type than its medial axis. In *Proc. ACM Symposium on Solid Modeling and Applications* (2003), pp. 65–75.

[LM03] LIN M., MANOCHA D.: Collision and proximity queries. In *Handbook of Discrete and Computational Geometry* (2003).

[Mil93] MILENKOVIC V.: Robust construction of the Voronoi diagram of a polyhedron. In *Proc. 5th Canad. Conf. Comput. Geom.* (1993), pp. 473–478.

[PG90] PATRIKALAKIS N. M., GÜRSOY H. N.: Shape interrogation by medial axis transform. In *Proc. 16th ASME Design Automation Conference* (Sept. 1990).

[PSS*03] PIZER S. M., SIDDIQI K., SZEKELY G., DAMON J. M., ZUCKER S. W.: Multiscale medial loci and their properties. *International Journal of Computer Vision 55* (2003), 155–179.

[RT95] REDDY J., TURKIYYAH G.: Computation of 3D skeletons using a generalized Delaunay triangulation technique. *Computer-Aided Design 27* (1995), 677–694.

[SA95] SHARIR M., AGARWAL P. K.: *Davenport-Schinzel Sequences and Their Geometric Applications*. Cambridge University Press, New York, 1995.

[SERB98] SHEFFER A., ETZION M., RAPPOPORT A., BERCOVIER M.: Hexahedral mesh generation using the embedded voronoi graph. *7th International Meshing Roundtable* (1998), 347–364.

[SFM05] SUD A., FOSKEY M., MANOCHA D.: Homotopy preserving medial axis simplification. In *Proc. ACM Symposium on Solid and Physical Modeling* (2005).

[SGG*06] SUD A., GOVINDARAJU N., GAYLE R., KABUL I., MANOCHA D.: Fast proximity computation among deformable models using discrete voronoi diagrams. *ACM Trans. Graph. (Proc ACM SIGGRAPH) 25*, 3 (2006), 1144–1153.

[SGGM06] SUD A., GOVINDARAJU N., GAYLE R., MANOCHA D.: Interactive 3d distance field computation using linear factorization. In *Proc. ACM Symposium on Interactive 3D Graphics and Games* (2006), pp. 117–124.

[She95] SHERBROOKE E. C.: *3-D Shape Interrogation by Medial Axis Transform*. Ph.D. thesis, Dept. Ocean Engineering, Massachusetts Institute of Technology, Cambridge, Massachusetts, 1995.

[SOM04] SUD A., OTADUY M. A., MANOCHA D.: DiFi: Fast 3D distance field computation using graphics hardware. *Computer Graphics Forum (Proc. Eurographics) 23*, 3 (2004), 557–566.

[Spa89] SPANIER E. H.: *Algebraic Topology*. Springer, 1989.

[SPB96] SHERBROOKE E. C., PATRIKALAKIS N. M., BRISSON E.: An algorithm for the medial axis transform of 3d polyhedral solids. *IEEE Trans. Visualizat. Comput. Graph. 2*, 1 (Mar. 1996), 45–61.

[SS06] STOLPNER S., SIDDIQI K.: Revealing significant medial structure in polyhedral meshes. In *Third International Symposium on 3D Data Processing, Visualization and Transmission* (2006).

[Sug92] SUGIHARA K.: Algorithms for computing Voronoi diagrams. In *Spatial Tesselations: Concepts and Applications of Voronoi Diagrams*, Okabe A., Boots B., Sugihara K., (Eds.). John Wiley & Sons, Chichester, UK, 1992.

[Sur03] SURESH K.: Automating the CAD/CAE dimensional reduction process. In *Proc. ACM Symposium on Solid Modeling and Applications* (2003), pp. 76–85.

[TH03] TAM R., HEIDRICH W.: Shape simplification based on the medial axis transform. *IEEE Visualization* (2003).

[TT97] TEICHMANN M., TELLER S.: *Polygonal Approximation of Voronoi Diagrams of a Set of Triangles in Three Dimensions*. Tech. Rep. 766, Laboratory of Computer Science, MIT, 1997.

[VO98] VLEUGELS J., OVERMARS M. H.: Approximating Voronoi diagrams of convex sites in any dimension. *International Journal of Computational Geometry and Applications 8* (1998), 201–222.

[Wol92] WOLTER F. E.: *Cut Locus and Medial Axis in Global Shape Interrogation and Representation*. Tech. Rep. 92-2, MIT, Dept. Ocean Engg., Design Lab, Cambridge, MA 02139, USA, Jan. 1992.